

electric and magnetic field. During their motion they create new electron-ion pairs by electron impact ionization until their energy is below the ionization threshold energy. The electrons created in such way have (except when they are generated in the cathode sheath) low energy. Although they outnumber by far the amount of HEE, we will neglect these low energy electrons in our model.

As mentioned in the introduction, we assume a 2D geometry. To further simplify the geometry, we limit ourselves to one side of the racetrack as indicated by the cross section in the upper left corner of Figure 1. The magnet system is determined by two magnets with opposite polarization, placed on a yoke and with distance d between their centers. The target thickness is given by z_0 . For the simulations we assume a flat target, i.e., the effect of the formation of the erosion profile is not taken into account. The magnetic field \mathbf{B} is calculated analytically by introducing magnetic charges [3]. The electric field \mathbf{E} is calculated by assuming that \mathbf{E} varies linearly from its maximum absolute value at the target surface to zero at a distance d_E above the target. Hence, the electric field is characterized by the discharge voltage V_d and the thickness of the cathode sheath d_E . The problem of determining the values of V_d and d_E is discussed in the subsection Self-consistency.

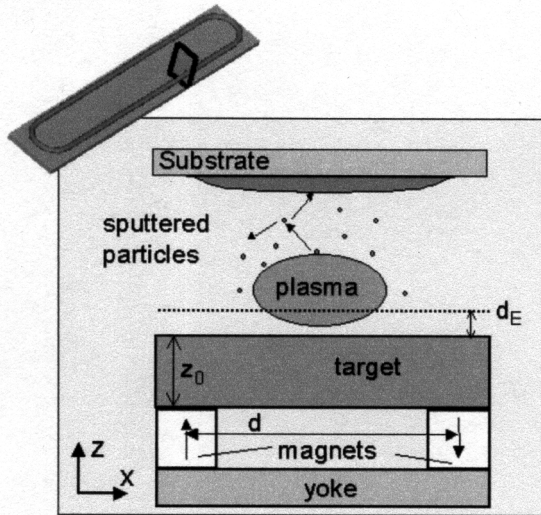


Figure 1: This sketch shows the 2D model used for the simulations. The magnet system consists of two magnets of equal strength (B) but with opposite magnetization directions, placed on a yoke. The distance between the two centers of the magnets is characterized by d , the target thickness by z_0 and the cathode fall by d_E . The inset in the upper left corner shows which part of the rectangular magnetron the model represents.

We now discuss briefly the model we developed for the planar DC magnetron discharge. A more detailed and mathematically founded description can be found in Reference 4.

Discharge Characterization

In a sufficiently strong magnetic field the movement of the HEE between two interactions follows arch-shaped regions that are determined by the magnetic field. Therefore, we consider the discharge as built up by these arches A_i in such a way that each arch corresponds with a position x_i along the x -axis on the target surface (Figure 2). The spatial distribution of the HEE [5] and also their energy distribution [6] is, to a good approximation, homogenous in these arches. However, corrections to these distributions in the sheath are needed [4].

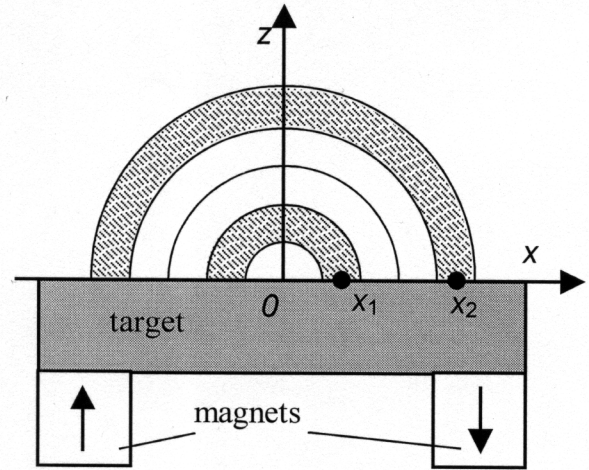


Figure 2: Sketch showing how the discharge can be considered as built up by arches. Each arch has a corresponding position on the target surface. This sketch is an idealization because the arches are concentric circle segments, which is not the case for a realistic magnet system. Arches corresponding with x -positions close to the center of the racetrack (e.g., x_1) are referred to as inner arches, arches corresponding with x -positions towards the edge of the race track (e.g., x_2) are referred to as outer arches.

By splitting up the discharge in arches, we can characterize the normalized HEE distribution of the discharge by a vector u : each element of u gives for the corresponding x -position the probability that a HEE of the discharge is located in the arch connected with that x -position. We will refer to this vector u as the occupation profile. Using this terminology, the normalized distribution of HEE (H) in the discharge is given by:

$$H = \sum_i u_i A_i$$

Eq. 1

As a good approximation, the normalized ionization distribution I can be assumed to be proportional with H [4].

We also introduce the emission profile r : each element of this vector gives the probability of a SE being emitted from the target at the corresponding x -position. Similarly, we define the erosion profile w : each element of this vector gives the probability that an atom sputtered from the target is sputtered at the corresponding x -position.

Motion of the HEE

This part of the model deals with the motion and the ionization of the HEE in the discharge. Solving this problem is equivalent to answering the question: where does a SE emitted at a position x_0 along the x -axis ionize in the discharge? The standard way to address this question is to combine the numerical solution of the Lorentz equation of motion

$$\frac{d\mathbf{v}}{dt} = \frac{q}{m}(\mathbf{E} + \mathbf{v} \times \mathbf{B})$$

Eq. 2

(q , m and v the electric charge, mass and velocity of the electron, respectively) with a Monte Carlo method to describe the electron interactions with the discharge gas. This requires the knowledge of the gas pressure (p) and both the magnetic and electric field. Also the cross sections for the different processes (ionization, excitation and elastic collisions) are needed. We performed these calculations, using the cross sections found in [7] and the algorithm described in [8]. The result for SE emitted at $|x|=2\text{mm}$ and at $|x|=10\text{mm}$ for a magnet system defined by $d=36\text{mm}$, $z_0=15\text{mm}$ and $B_r=0.7\text{T}$ is shown in Figure 3.

Because this kind of Monte Carlo simulation is very time consuming, we developed an alternative approach based on the splitting up of the discharge as shown in Figure 2. In this approach, the influence of an interaction of a HEE is interpreted as a transfer probability for the HEE to move from one arch shaped region to another. This probability is determined by the Larmor radius of the HEE and by the distance between the two arches. The probability t_{ij} that a HEE in arch j is transferred to arch i is calculated for all possible arches i and j . This way a square matrix \mathbf{T} , called the transfer matrix, with elements t_{ij} is constructed. It can be shown [4] that the probability that a HEE is transferred from arch j to arch i after m interactions is given by element i,j from the matrix \mathbf{T}^m (the matrix \mathbf{T} to the power m).

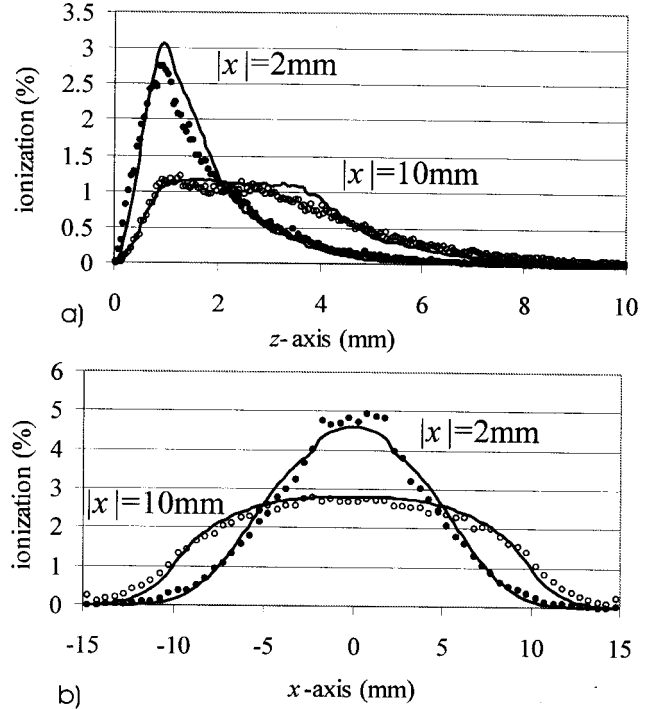


Figure 3: Plots of the normalized ionization distribution integrated along the x -axis (a) and the along the z -axis (b) for a SE emitted at $|x|=2\text{mm}$ and 10mm . The magnet system used for these calculations is defined by $d=36\text{mm}$, $B_r=0.7\text{T}$ and $z_0=15\text{mm}$. Furthermore we set $V_d=-300\text{V}$ and $p=0.5\text{Pa}$. The results represented by the dots are obtained with the Monte Carlo method, the ones represented by the solid line with our alternative method [4].

If one takes a single SE, which is emitted at a certain x -position, all elements of the emission profile r are zero except for the element corresponding with the starting position of the SE, which will be one. As long as the SE does not undergo an interaction, the occupation profile u will be equal to the emission profile r . However, after a certain time the SE will interact with the target or with the discharge gas, whatever occurs first. If it interacts with the discharge gas, u will no longer be equal to r but will be determined by:

$$u = \mathbf{T}r$$

Eq. 3

After two interactions with the discharge gas, u will be given by

$$u = \mathbf{T}^2 r$$

Eq. 4

and so on. If at interaction n the energy of the HEE drops below the ionization threshold, i.e., the electron is no longer a HEE, the average occupation profile u_{avg} is given by

$$u = \mathbf{T}_{avg} r \quad \text{Eq. 5}$$

with \mathbf{T}_{avg} the average of unit matrix and the matrices $\mathbf{T}, \mathbf{T}^2, \dots, \mathbf{T}_{n-1}$ [4].

If the SE is recaptured by the target, it does not contribute to the discharge. This recapture reduces the effective SE yield γ and is very important because it is strongly pressure dependent. The probability that a SE interacts with the discharge gas, i.e., that it is *not* recaptured, is given by [9]:

$$f = 1 - e^{-\frac{s}{\lambda}} \quad \text{Eq. 6}$$

with s the distance a SE would travel before it is recaptured by the target if there would be no discharge gas, and λ the mean free path length of the SE in the discharge. Because of the recapture probability, Equation 5 needs to be adapted. Furthermore, a HEE can also ionize in the cathode sheath. In that case, the newly generated electron can also be accelerated into the discharge and become a HEE. Also this effect needs to be taken into account in Equation 5 for an accurate deduction of u from r . We conclude that, although the relationship is more complicated as Equation 5, the occupation profile u can be derived from the emission profile r . From this u , the normalized distributions H and I can be determined (Equation 1).

Using this method we calculated the ionization distribution for the same conditions and for the same SE ($|x|=2$ and 10mm) as for the Monte Carlo method. The results are given in Figure 3. The two ionization distributions agree well in both the direction perpendicular to the target surface (z -axis) as well as in the direction along the target surface (x -axis). We conclude that using our method, the normalized ionization distribution can be calculated in a fraction of the time needed by the Monte Carlo method without losing too much accuracy.

Discharge Model

To simulate the whole discharge, we assume a certain emission profile r ; this means we assume that we know for each position along the x -axis the number of SE that are emitted. To find the ionization that results from this r we apply the procedure as described in the previous subsection. The next step of the model is to determine the amount of newly emitted SE, i.e., the new emission profile r' , evoked by this ionization

distribution. Therefore, we assume that the ions reach the target without undergoing any collisions and that all created ions are accelerated towards the target. Given the typical low gas pressures used in magnetron discharges (order of 0.5Pa) the first assumption poses no problem. The second assumption requires some explanation. Ions formed in the cathode sheath, i.e., in the region within distance d_E above the target surface, feel the (strong) electric field in the sheath and are accelerated towards the target. Ions formed above the cathode sheath do not feel an electric field in our simplified model. However, in reality there is a small presheath to satisfy the Bohm criterion [10]. For calculating the HEE movement, this sheath has very little influence, which is the reason for neglecting it. For the ions, however, this small electric field guarantees that all ions are accelerated towards the target. Hence, summing all the ions and multiplying this number with the SE yield γ , which gives the amount of SE emitted per incoming ion, results in new emission profile r' .

Self-consistency

Given the previous subsection, we can translate the processes occurring to sustain the discharge into the model formalism. We assume a certain distribution of SE emitted from the target, which is represented in the model by assuming an emission profile r . These emitted SE become the HEE of the discharge and cause the ionization. In the model this means that the emission profile r is converted into the occupation profile u . From this u we can deduce the normalized HEE distribution H and ionization distribution I (Equation 1). The formed ions bombard the target and this causes the release of new SE, which means in the model that we derive from I a new r' .

It is clear that for a steady-state condition r and r' should be equal. Hence, the whole procedure for determining r' from a given r is iterated until this condition is satisfied. It appears that for a given V_d, d_E and magnet system this condition can only be satisfied for one specific gas pressure p . It can be shown that for the given discharge voltage V_d and magnet system, the pressure for which V_d is the minimum discharge voltage needed to sustain the plasma discharge is found [4]. This is one of the limitations of the model as it means that for a given discharge voltage V_d there is only a solution for one specific pressure. In reality, there is a range of pressures possible for a given V_d . This is one of the topics we are currently working on.

Now we also tackle the problem of determining d_E , the cathode fall thickness, as this discharge property was so far chosen arbitrarily. According to the simulations performed by Nanbu and Kondo [11], the height above the target where the ionization rate is maximum and the height where the electric field becomes practically zero are almost equal to each other. Now, for an initial arbitrarily choice of d_E this condition will not be satisfied. Hence, the whole procedure described above

has to be repeated until this condition also is satisfied. This way we find a self-consistent value for d_E .

Deducing the Erosion Profile

Once a self-consistent steady-state condition is found, the erosion profile w on the target can be deduced. Therefore, we use the same assumptions as for deducing r' from I , namely that the ions reach the target without undergoing any collisions and that all ions, also the ones created above the cathode sheath, reach the target. Instead of the SE yield γ we need here the sputter yield Y , which gives the amount of sputtered particles per incoming ion. As the sputter yield is energy dependent, we need to take it into account as a weight factor when summing over the ion distribution.

PRESSURE DEPENDENCE OF THE MAGNETRON DISCHARGE

For the discussion of the pressure dependence of the magnetron discharge, we will focus on the discharge voltage and on the erosion profile, because these two properties are very important for determining the deposition profile [2]. For obtaining the simulation results, we used the same magnet system as for the results shown in Figure 3. The experiments were performed with a commercially available magnetron (Von Ardenne type PPS50) with an enlarged aluminum target (diameter 58mm) [3]. The simulations give for each discharge voltage the pressure for which the given discharge voltage is the minimum discharge voltage to sustain the discharge (see subsection *Self-consistency*). As this situation is difficult to achieve experimentally, we chose to work in constant (low) current mode. The configuration used for the simulations is chosen to represent a "typical" magnetron configuration and is not meant as a perfect model of the real magnetron used. Hence, we cannot expect exact agreement between the simulation results and the experimental results. Our aim is to show that, in spite of the simplifications, our model simulates correctly the pressure dependence of the discharge.

Figure 4 shows the width of the erosion profile as a function of gas pressure. We see that down to gas pressures of approximately 0.5Pa (5.10-3mbar) the full width at half maximum (FWHM) increases very slowly. Below this pressure, however, the FWHM increases rapidly. It can be seen that the FWHM almost doubles in the shown pressure range. Hence, the change of the erosion profile with pressure can be important. Last year, we presented experimental measurements of the pressure dependence of the erosion profile [3]. These experimental results are also shown in Figure 4. Note that because of the difference in magnetron geometry between the simulation and experiments, the absolute width of the erosion profiles is different. On relative terms their pressure behavior shows the same tendency, though.

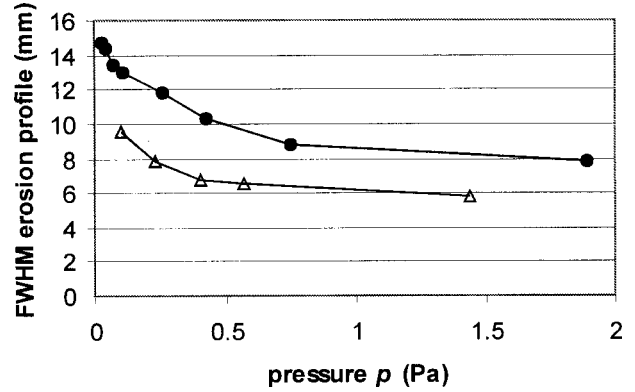


Figure 4: Full width at half maximum (FWHM) of the erosion profile as a function of gas pressure p . The dots represent simulation results, the open triangles the experimental measurements.

Figure 5 shows the pressure dependence of the discharge voltage. It contains also the experimental result obtained for a constant current of 0.25A and for a target thickness of 2mm [12]. Again, we see that the calculations express the same general trend as the experiments.

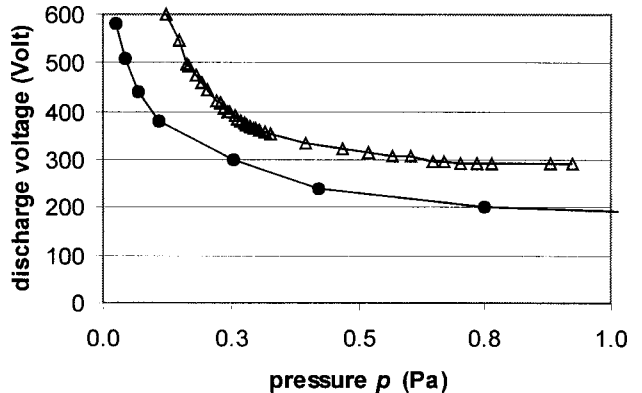


Figure 5: Discharge voltage V_d as a function of gas pressure p . The dots represent simulation results, the open triangles the experimental measurements.

Because our model is based on splitting up (dissecting) the magnetron discharge, we can now very well retrace the origin of this pressure dependence. By investigating each individual step of the model, we found that the recapture of the SE is influenced the strongest by the pressure. This is expressed by the mean free path length l in Equation 6. Because of this recapture, the number of SE created per ion that participate in the discharge is decreased. The average probability f_{avg} (defined as the average of f over the race track) that a SE emitted at the target effectively takes part in the discharge is given in Figure 6 as a function of pressure p . As the effect of recapture of SE can be interpreted as a reduction of the SE yield, the

effective SE yield as seen by the discharge will be proportional with f_{avg} . According to Thornton [13], the minimum discharge voltage is inversely proportional with the effective SE yield. Hence, V_d is proportional with $1/f_{avg}$. This explains the increase of the discharge voltage with decreasing gas pressure as shown in Figure 5. It is important to note that the escape of HEE out of the trap formed by the electric and magnetic field did *not* appear as a main reason for the pressure dependence. Hence, the reasoning that with decreasing pressure more and more energetic electrons escape from the discharge region and that this leads to an increase in the discharge voltage appears to be wrong.

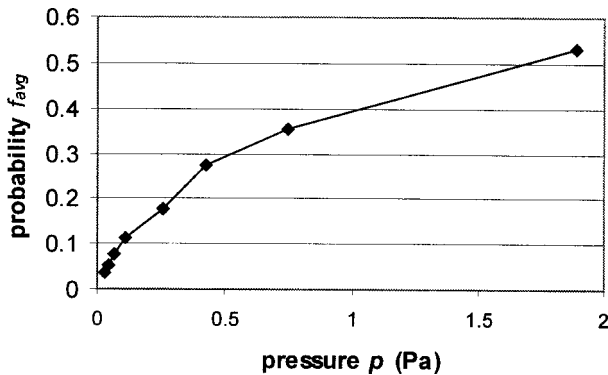


Figure 6: The average probability f_{avg} that a SE emitted at the target surface interacts with the discharge gas as a function of pressure.

The widening of the erosion profile can also be explained in this fashion. First of all, the increased recapture of SE with decreasing pressure is the strongest for the SE emitted near the center of the racetrack [3]. This means that relatively more SE will be emitted from the edges of the racetrack at low pressures, and hence, the outer arches will be relatively more occupied. As these arches are spread more than inner arches (Figure 2), this causes a widening of the erosion profile. Furthermore, because of the increased discharge voltage, the HEE can undergo more interactions before their energy drops below the ionization threshold energy. As they are the interactions that enable the HEE to transfer across the arches, the more interactions a HEE can undergo, the higher the probability that it will reach outer arches. This adds to the widening of the erosion profile.

CONCLUSION

In this article we presented a model for the DC planar magnetron discharge that is based on separating as much as possible the different processes occurring in the discharge. The reason for this dissection of the discharge is that it allows to gain insight in the relative importance of the different discharge processes, to simplify these different processes and to focus on the discharge properties that are important for controlling the film deposition.

It also allowed us to develop an alternative method for determining the ionization distribution of the HEE in the discharge which is much quicker than the standard method (Monte Carlo simulations). However, our method is only valid for sufficiently strong magnetic fields and for 2D geometries (no end effects). By comparing our results with Monte Carlo calculations, we showed the validity of our approach.

Using our model, we simulated the pressure dependence of a “typical” magnetron discharge. Comparison with experimental observations shows that the general trend of the pressure dependence of both the erosion profile and the discharge voltage could be simulated. It appears that the main cause for the pressure dependence is the increased recapture of secondary electrons by the target with decreasing gas pressure.

ACKNOWLEDGMENT

This research is financed with a grant from the Institute for the Promotion of Innovation by Science and Technology in Flanders (IWT).

REFERENCES

1. C.H. Shon and J.K. Lee, “Modeling of Magnetron Sputtering Plasmas,” *Appl. Surf. Sci.* 192, 258, 2002.
2. W. De Bosscher, A. Blondeel and G. Buyle, “Uniformity Control in Sputter Deposition Processes”, 45th Annual Technical Conference Proceedings of the Society of Vacuum Coaters, p. 135, 2002.
3. G. Buyle, D. Depla, K. Eufinger, J. Haemers, W. De Bosscher, and R. De Gryse, “Influence of Recapture of Secondary Electrons on the Magnetron Sputtering Deposition Process,” 45th Annual Technical Conference Proceedings of the Society of Vacuum Coaters, p. 348, 2002.
4. G. Buyle, D. Depla, K. Eufinger, J. Haemers, W. De Bosscher and R. De Gryse, “Simplified Model for Calculating the Pressure Dependence of a DC Planar Magnetron Discharge,” submitted.
5. A. E. Wendt, M. A. Lieberman, and H. Meuth, “Radial Current Distribution at a Planar Magnetron Cathode,” *J. Vac. Sci. Technol. A* 6, 1827, 1988.
6. F. Guimarães, J. Almeida, and J. Bretagne, “Modeling of the Energy Deposition Mechanisms in an Argon Magnetron Planar Discharge,” *J. Vac. Sci. Technol. A* 9, 133, 1991.
7. M. Hayashi, set of cross-sections for electron-argon interaction, made available via the web site <http://jilaweb.colorado.edu/www/research/colldata.html> by A.V. Phelps.

-
8. A. Bogaerts, *Mathematical modeling of a direct current glow discharge in argon*. PhD Thesis, Universiteit Antwerpen, 1996.
 9. G. Buyle, W. De Bosscher, D. Depla, K. Eufinger, J. Haemers and R. De Gryse, "Recapture of secondary electrons by the target in a DC planar magnetron discharge," *Vacuum*, 70, 29, 2003.
 10. B. Chapman, *Glow Discharge Processes*, p. 65-70, WILEY, New York, 1980.
 11. S. Kondo, and K. Nanbu, "A self-consistent numerical analysis of a planar dc magnetron discharge by the particle-in-cell/Monte Carlo method," *J. Phys. D: Appl. Phys.* 32, 1142, 1999.
 12. J. Lei et al, to be published.
 13. J.A. Thornton, "Magnetron sputtering: basic physics and application to cylindrical magnetrons," *J. Vac. Sci. Technol.*, 15 (2), 171, 1978.